Journal of Colloid and Interface Science **243,** 280–291 (2001)
doi:10.1006/jcis.2001.7796, available online at http://www.idealibrary.com on IDEAL®

Adsorption of Copper(II) onto Perlite

Mahir Alkan*,[1] and Mehmet Doğan†

*Department of Chemistry, Necatibey Education Faculty, and †Department of Chemistry, Faculty of Science and Literature, Balıkesir University, 10100 Balıkesir, Turkey

E-mail: malkan@balikesir.edu.tr, mdogan@balikesir.edu.tr.

Received February 21, 2001; accepted June 22, 2001; published online October 5, 2001

Perlite samples activated by H_2SO_4 solutions were utilized as adsorbents for the removal of Cu(II) ions from solutions at different pHs, ionic strengths, and temperatures. It has been found that the amount of Cu(II) adsorbed increased with increased pH, whereas it decreased as the ionic strength, temperature, and acid activation increased. Adsorption isotherms correlated reasonably well with the Langmuir adsorption isotherm and Langmuir parameters of adsorption isotherm (Q_m and K) were found with the aid of the linearized Langmuir isotherm. The entalphy change for Cu^{2+} adsorption has been estimated as -5.14 ± 1 and 4.38 ± 1 kJ/mol for unexpanded and expanded perlite samples, respectively. Proton stoichiometry (x) was calculated from Kurbatov plot using the amount of Cu(II) adsorbed at different pH. The dimensionless separation factor (R) has shown that perlite can be used for removal of Cu(II) ion from aqueous solutions, but unexpanded perlite is more effective.

Key Words: **Copper; perlite; adsorption isotherms; metal ion; proton stoichiometry.**

1. INTRODUCTION

The adsorption of heavy metal cations onto oxide surfaces has been the subject of many studies in recent years. The presence of metals in aquatic environments has been known to cause several health problems in animals and human beings (1, 2). Heavy metal levels in waste water, drinking water, and water used for agriculture must be reduced to a maximum permissible concentration. Precipitation, ion exchange, solvent extraction, and adsorption on oxides are the conventional methods for the removal of heavy metal ions from aqueous solutions (1, 3–6), but due to high maintenance cost these methods do not suit the needs of developing countries (1, 7).

The adsorption process is used especially in the water treatment field and investigation has been made to determine good, inexpensive adsorbents. Studies so far have focused on adsorbents such as alumina (8–10), magnetite (8, 11), pyrolusite (8), rutile (9, 12), zirconia (9), hydrous manganese oxide (13), silica (14–18), geothite (19–23), heamatite (24), amorphous ferric oxide (25), bentonite (1, 26), activated carbon (27), sphalerite (28, 29), anatase (30, 31), red mud (32, 33), mica (34), illite (35), kaolinite (36), and clay (37).

Perlite is a glassy volcanic rock, commonly light gray, with a rhyolitic composition and 2 to 5% combined water (38). Expanded perlite meets competition from various other industrial minerals (39). Commercially, the term perlite includes any volcanic glass that will expand or "pop" when heated quickly, forming a lightweight frothy material. The temperature at which expansion takes place ranges from 760 to 1100°C; a volume increase of 10 to 20 times is common (38). However, this versatile, lightweight material with its low bulk density continues to grow in popularity even though it is by no means the cheapest (39). Along the Aegean coast, Turkey possesses about 70% (70×10^9 tons) of the world's known perlite reserves (40). The uses of expanded perlite are many and varied and are based primarily upon its physical and chemical properties. Because of their low thermal conductivity, high adsorption of sound, low bulk density, and fire resistance, perlite aggregate plasters hold many advantages over conventional plaster. Over half of the perlite produced goes into the construction industry, in particular as aggregate in insulation board, plaster, and concrete. In cryogenic (extremely low temperature) applications, perlite is used to insulate storage vessels for liquefied gas. Expanded perlite is used as a rooting medium and soil conditioner, and as a carrier for herbicides, insecticides, and chemical fertilizers. Accurately sized perlite is used as an aid in filtering water and other liquids, in food processing, and in pharmaceutical manufacture. As most perlites have a high silica content, usually greater than 70%, and are adsorptive, they are chemically inert in many environments and hence are excellent filter aids and fillers in various processes and materials. Miscellaneous uses of expanded perlite include fillers or extenders in paints, enamels, glazes, plastics, resins, and rubber, as a catalyst in chemical reactions; as an abrasive; and as an agent in mixtures for oil well cementing (41).

In our previous works, we investigated the electrokinetic properties (42) and surface titration of perlite suspensions (43) and also the adsorption of methylene blue from aqueous solutions onto perlite samples (44). In the present study, removal of

[1] To whom correspondence should be addressed.

0021-9797/01 $35.00

TABLE 1
Chemical Composition of Perlite

Constituent	Percentage present
SiO_2	71–75
Al_2O_3	12.5–18
Na_2O	2.9–4.0
K_2O	4.0–5.0
CaO	0.5–2.0
Fe_2O_3	0.1–1.5
MgO	0.03–0.5
TiO_2	0.03–0.2
MnO_2	0.0–0.1
SO_3	0.0–0.1
FeO	0.0–0.1
Ba	0.0–0.1
PbO	0.0–0.5
Cr	0.0–0.1

Cu^{2+} from aqueous solutions by adsorption has been studied. The effects of solution pH, ionic strength, acid activation, and temperature on Cu^{2+} adsorption have been evaluated and the proton stoichiometry and parameters for Langmuir adsorption isotherms have been reported. The results obtained have been applied to a batch design for the removal of Cu^{2+} ions from aqueous media using perlite samples.

2. MATERIALS AND METHODS

2.1. Materials

The unexpanded and expanded perlite samples were obtained from Cumaovası Perlite Processing Plants of Etibank (İzmir, Turkey). The chemical composition of the perlite found in Turkey in the literature is given in Table 1 (40). The unexpanded and expanded perlite samples were treated as follows (42) before being used in the experiments: the suspension containing 10 g/L perlite was mechanically stirred for 24 h; after about 2 min the supernatant suspension was filtered through a white-band filter paper ($\Phi = 12.5$ cm). The solid sample was dried at 110°C for 24 h, then sieved by a 100-mesh sieve. The particles under 100-mesh were used in further experiments.

H_2SO_4 solutions were used to obtain the acid-activated perlite samples. The aqueous suspensions of both the unexpanded and expanded perlite samples in 0.2, 0.4, and 0.6 M H_2SO_4 solutions (so the acid/solid ratios were 1/5, 2/5, and 3/5 g/g) were refluxed with a reflux apparatus, filtered and washed with distilled water until no precipitation was observed upon the addition of $Ba(aq)^{2+}$ into the filtrate, and finally dried at 110°C for 24 h.

The cation exchange capacity (CEC) of the various perlite samples was determined by the ammonium acetate method; density by the pyknometer method. The specific surface area of the samples of expanded perlite (EP), acid-activated expanded perlite (EHP(0.6)), unexpanded perlite (UP), and acid-activated unexpanded perlite (UHP(0.6)) were measured by BET N_2 adsorption. The results are summarized in Table 2 (42). All chemicals were obtained from Merck.

2.2. Methods

Adsorption experiments were carried out in 100-mL polyethylene flasks by shaking 0.5-g perlite samples with various amounts of stock Cu^{2+} solutions prepared from $CuCl_2 \cdot 2H_2O$ and standardized titrimetically at 30°C, natural solutions pH (6.1 ± 0.3), and constant ionic strength (0.2 M NaCl), except those in which varying conditions of temperature, pH, and ionic strength were investigated. The concentration of Cu^{2+} solutions for both sets of perlite samples was varied in the range of 1.6×10^{-5}–2.4×10^{-4} mol/L. A preliminary experiment revealed that about 15 h is required for Cu^{2+} ions to reach the equilibrium concentration. The flasks were shaken mechanically for 15 h at 30 ± 0.2°C. The solution was filtered through Whatmann 42 filter paper. The pH of the solution was measured and considered as the equilibrium pH. Each run was made at least in duplicate. A thermostated shaker bath was used to keep the temperature constant. The pH of the solution was adjusted with NaOH or HNO_3 solution by using an Orion 920A pH meter with a combined pH electrode. The pH meter was standardized with NBS buffers before every measurement. The concentration of Cu^{2+} ions in the filtrate was determined by AAS (Unicam 929). Blanks containing no Cu^{2+} were used for each series of experiments. The amounts of Cu^{2+} adsorbed were calculated from the concentrations in solutions before and after adsorption (44).

TABLE 2
Some Physicochemical Properties of Perlite Samples Used in the Study

Sample	Nomenclature	CEC (meg/100g)	Density (g/mL)	Specific surface area (m^2/g)	Zeta potential (mV)
Expanded, purified in water	EP	33.30	2.24	2.30	−46.8
Expanded, 0.2 M acid-activated	EHP(0.2)	38.20	2.10	—	−47.1
Expanded, 0.4 M acid-activated	EHP(0.4)	43.38	2.04	—	−46.3
Expanded, 0.6 M acid-activated	EHP(0.6)	54.24	1.93	2.33	−44.0
Unexpanded, purified in water	UP	25.97	2.30	1.22	−23.5
Unexpanded, 0.2 M acid-activated	UHP(0.2)	32.79	2.32	—	−21.8
Unexpanded, 0.4 M acid-activated	UHP(0.4)	35.00	2.38	—	−22.0
Unexpanded, 0.6 M acid-activated	UHP(0.6)	36.56	2.46	1.99	−21.1

3. RESULTS AND DISCUSSION

3.1. Proton Stoichiometry

Several authors have investigated the overall stoichiometry of surface complex formation by measuring the number of hydrogen ions released per adsorbed metal ion. Since specific adsorption of multivalent cations almost always involves proton exchange, an important characteristic of the adsorption processes is the number of protons released, or hydroxide ions adsorbed, for each cation adsorbed (45). To identify the appropriate model of adsorption, as a first step it is necessary to determine the stoichiometry of the reaction (46), which characterizes the net H^+ exchange and varies with pH and the coverage of the surface with adsorbate (47). It has been observed that at concentrations of metal ions lower than 10^{-4} M, batch titration data yield a very high ratio of protons released M^{2+} adsorbed. Indeed, all the published data correlating $(C_B - C_A)$ with $[M^{2+}]$ are in the M^{2+} concentration range 10^{-3}–10^{-4} M. Therefore, the titrimetric method is not suitable for determining the stoichiometry of the reaction at low concentrations of metal ions (45). Fokkink and co-workers recently proposed a simple double-layer model for estimating the value of the proton coefficient. They predict a value for x in the range 1 to 2 under most experimental conditions, the particular result being determined primarily by $\Delta pH = (pH_{pzc} - pH)$, where pH_{pzc} is the point of zero charge (23, 48). It has been shown by Doğan *et al.* (42) that the perlite samples have no point of zero charge and exhibit negative zeta potential values in the pH range 3–11. Therefore, this method is not suitable for calculating x from experimental data. As an alternative method one may use the mass law expression to determine the stoichiometry of the surface interaction and this has proved to be a useful empirical approach (45, 46).

The adsorption of copper(II) can be expressed according to the following equations given by Park *et al.* (49) and Bourg and Schindler (50):

$$\mathrm{SiOH} + \mathrm{Cu^{2+}} \rightleftharpoons \mathrm{SiO{-}Cu^{+}} + \mathrm{H^{+}}, \qquad [1]$$

$$K_1 = \frac{[\mathrm{SiO{-}Cu^{+}}][\mathrm{H^{+}}]}{[\mathrm{SiOH}][\mathrm{Cu^{2+}}]}; \qquad [2]$$

$$\mathrm{SiOH} + \mathrm{Cu^{2+}} + \mathrm{H_2O} \rightleftharpoons \mathrm{SiO{-}CuOH^{0}} + 2\,\mathrm{H^{+}}, \qquad [3]$$

$$K_2 = \frac{[\mathrm{SiO{-}CuOH^{0}}][\mathrm{H^{+}}]^2}{[\mathrm{SiOH}][\mathrm{Cu^{2+}}]}; \qquad [4]$$

$$2\,\mathrm{SiOH} + \mathrm{Cu^{2+}} \rightleftharpoons (\mathrm{SiO})_2\mathrm{Cu^{0}} + 2\,\mathrm{H^{+}}, \qquad [5]$$

$$K_3 = \frac{[(\mathrm{SiO})_2\mathrm{Cu^{0}}][\mathrm{H^{+}}]^2}{[\mathrm{SiOH}]^2[\mathrm{Cu^{2+}}]}. \qquad [6]$$

If $[Cu^{2+}]_{ads}$ represents the adsorbed amount of copper(II) in terms of any one of the reactions [1], [3], or [5], the equations below can be written

$$\log \frac{[\mathrm{Cu^{2+}}]_{ads}}{[\mathrm{Cu^{2+}}]_e} = [\log K_1 + \log(\mathrm{SiOH})] + \mathrm{pH} \qquad [7]$$

or

$$\log \frac{[\mathrm{Cu^{2+}}]_{ads}}{[\mathrm{Cu^{2+}}]_e} = [\log K_2 + \log(\mathrm{SiOH})] + 2\mathrm{pH} \qquad [8]$$

or

$$\log \frac{[\mathrm{Cu^{2+}}]_{ads}}{[\mathrm{Cu^{2+}}]_e} = [\log K_3 + 2\log(\mathrm{SiOH})] + 2\mathrm{pH}, \qquad [9]$$

where $[Cu^{2+}]_e$ is the equilibrium concentration of Cu^{2+} in solution and [SiOH] is the concentration of active site of the surface.

A plot of the left-hand side of Eqs. [7], [8], or [9] versus equilibrium pH of the solution should yield a linear relationship, the slope of which gives the stoichiometric coefficient of the reactions [1], [3], or [5] (46). This plot, which is called a Kurbatov plot, is useful for two reasons. First, it is frequently linear for trace divalent cation adsorption. Second, one of these parameters—the slope of the plot—gives an indication of the stoichiometry of the H^+–M^{n+} exchange reaction if adsorption is at very low surface coverages and low solution concentrations. No other method is suitable for determination of this stoichiometry under these conditions (45).

The plots of $\log([Cu^{2+}]_{ads}/[Cu^{2+}]_e)$ versus equilibrium pH are shown in Fig. 1. From the slope of each line in Fig. 1, it has been found that the number of protons released per Cu^{2+} ion adsorbed onto perlite samples is 1.08 and 0.98 for unexpanded and expanded perlites, respectively. x values for different adsorbents and metal ions are given in Table 3. This result indicates that the adsorption of copper(II) from aqueous solution onto perlite surface occurs according to reaction [1]. The fact that the x values are about 1 for Cu^{2+} ion adsorption means that the surface charge becomes increasingly positive, as the Cu^{2+} ions in the solution are adsorbed onto the perlite surface, according to reaction [1].

3.2. Adsorption Isotherms

The surface hydroxyl groups of the adsorbent have the main effect on the adsorption of Cu^{2+} ion onto the perlite, so it would be useful to review the surface hydroxyl groups. The silicon atoms at the surface tend to maintain their tetrahedral coordination with oxygen. They complete their coordination at room temperature by attachment to monovalent hydroxyl groups, forming silanol groups. Theoretically, it is possible to use a pattern in which one silicon atom bears two or three hydroxyl groups, yielding silanediol and silanetriol groups, respectively. It is improbable that silanetriol groups exist at the silica surface. The type of silanol groups are shown below (42–44):

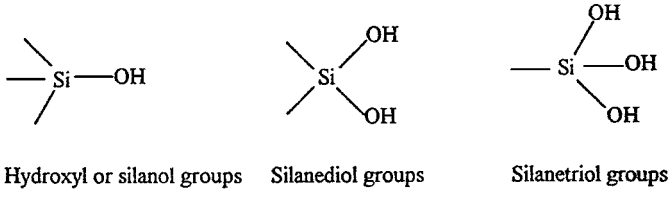

Hydroxyl or silanol groups Silanediol groups Silanetriol groups

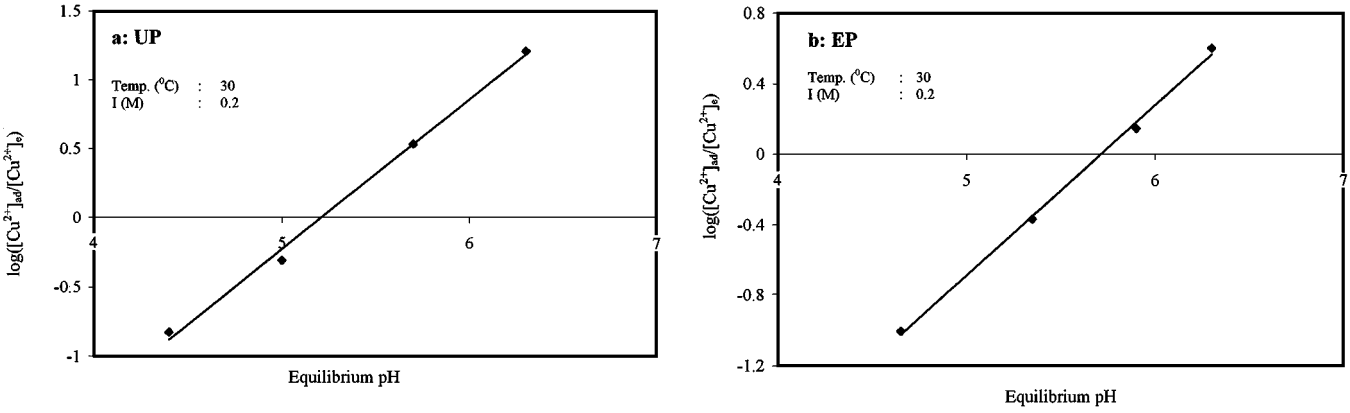

FIG. 1. Kurbatov plots for proton stoichiometry: (a) UP and (b) EP.

The hydrous oxide surface groups in alumina are as follows (42–44):

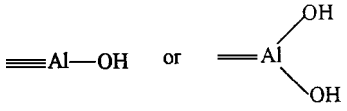

Adsorption of cations by hydrous metal oxides is frequently found to be extremely rapid, most of the exchange occurring within a matter of minutes. This rapid adsorption reflects the facts that the adsorption is a surface phenomenon and that the surfaces are readily accessible to the ions in solution. In microporous oxide systems, especially those obtained by heating, equilibrium is achieved somewhat more slowly (45). The rate of exchange is generally controlled by the rate of ion diffusion within the particle and this is related to the size, shape, and spatial distribution of the pores. The size distribution of micropores in hydrous oxides is frequently found to be very sensitive to heat treatment. The porosity and specific surface are generally found to reach a maximum at some particular temperatures, and then the specific surface area decreases with increasing temperature as a result of sintering (45). Figure 2 shows the adsorption isotherms of Cu^{2+} ions on the unexpanded and expanded perlite samples. The adsorbed amount of Cu^{2+} ions for unexpanded perlite is greater than that for expanded perlite. The decrease in the amount of adsorption by expansion may be a result of a decrease in the number of hydroxyl groups on the perlite samples during the calcination. The decrease in the number of hydroxyl groups of the adsorbent, which are the main effective sites for adsorption, during the expansion of perlite is thought to cause a decrease in adsorption capacity, although expanded perlite has greater values of cation exchange capacity (CEC), zeta potential (ZP), and specific surface area than unexpanded perlite (44).

The effect of acid activation on the adsorption of Cu^{2+} ions onto perlite samples is given in Fig. 3, which indicates that the numbers of adsorbed Cu^{2+} ions slightly decrease with the concentration of H_2SO_4 used for the acid activation for both of the perlite samples. This decrease observed may be due to the partial destruction of perlite structure as shown by Pradas *et al.* (52) and López-Gonzàlez and Gonzàlez-Garcìa (53) for bentonite, and also may be due to the decrease in OH groups in

TABLE 3
H^+ Released for Each Metal Ion Adsorbed onto Different Adsorbents

Adsorbent	Metal ion	x	References
δ-MnO_2	Pb^{2+}	1.4	(45)
	Cd^{2+}	1.3	(45)
	Zn^{2+}	1.1	(45)
	Tl^{+}	0.38	(45)
δ-MnO_2	Mn^{2+}	1.0–1.7[a]	(45)
	Co^{2+}	2.1 ± 0.26	(45)
	Zn^{2+}	2.1 ± 0.05	(45)
SiO_2	Ca^{2+}	1.0	(45)
	Co^{2+}	1.1–1.7[a]	(45)
	Fe^{2+}	1–2[a]	(45)
MnO_2	Mg^{2+}	0.05–0.25	(45)
	Ca^{2+}	0.12–0.35	(45)
MnO_2	Sr^{2+}	0.45	(45)
	Ba^{2+}	0.50	(45)
	Co^{2+}	1.03	(45)
	Mn^{2+}	0.90	(45)
	Ni^{2+}	1.18	(45)
	Zn^{2+}	0.14	(45)
Al_2O_3	Ca^{2+}	1.0–1.3[b]	(45)
	Pb^{2+}	1.5[b]	(45)
α-FeOOH	Cu^{2+}	1.5–2.0[a]	(45)
α-FeOOH	Cu^{2+}	2.4 ± 0.5	(45)
	Pb^{2+}	2.0 ± 0.5	(45)
	Co^{2+}	2.3 ± 0.6	(45)
α-FeOOH	Zn^{2+}	2.2 ± 0.3	(45)
Fe gel	Zn^{2+}	1.65	(45)
	Ca^{2+}	0.95	(45)
	Pb^{2+}	1.2–1.6[a]	(45)
Goethite	Cu^{2+}	1.66	(23)
Goethite	Cu^{2+}	1.1	(51)
UP	Cu^{2+}	1.08	This study
EP	Cu^{2+}	0.98	This study

[a] Increase with pH.
[b] No trend with pH.

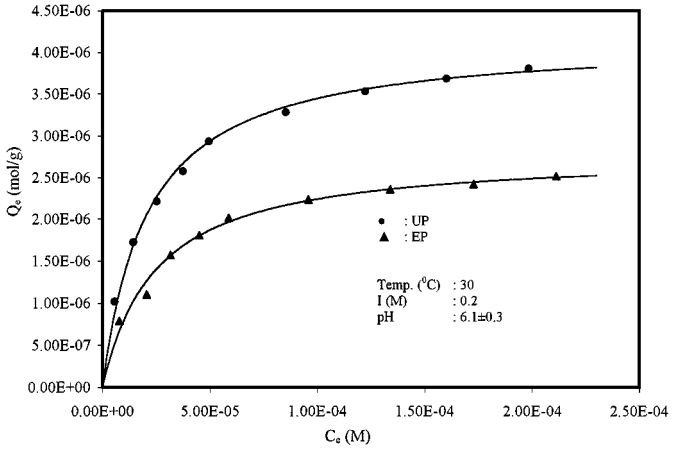

FIG. 2. The effect of thermal treatment on the adsorption of Cu^{2+} ions on perlite.

perlite during the activation process as was shown by Doğan (54) using IR spectra.

The tendency for multivalent cations to be adsorbed onto solid surfaces has also been put to use in scavenging impurities from solution and for the selective preconcentration of a number of trace elements. The hydrous metal oxides, particularly those of iron, aluminum, and manganese, have been used most frequently for these purposes, and the efficiency of removal of the metal ions from solution has invariably been found to be strongly pH dependent. A rapid increase in uptake of the metal ion usually occurs over a narrow pH range. This is particularly true for the strongly hydrolyzable cations (45) and has led many workers to view this uptake as an H^+–M^{2+} exchange reaction with the protons derived from the weakly acidic surface OH groups. To study the influence of pH on the adsorption capacity of perlite samples for Cu^{2+} ions, experiments were performed using various initial solution pH values from 5 to 7 (Fig. 4). It may be said that the adsorption capacity increases with increasing pH in the range of these pH values and that adsorption does not occur below pH 5. It has been shown (42) that the perlite samples have no point of zero charge and exhibit negative zeta potential value at the pH range 3–11:

$$-\mathrm{SiOH} + \mathrm{OH}^- \rightleftharpoons -\mathrm{SiO}^- + \mathrm{H_2O}, \qquad [10]$$

By taking into account that the x value for reaction [1] has been found to be equal to 1 as described in Section 3.1, it can be said that as the pH of Cu^{2+} solution becomes higher, the association of Cu^{2+} ions with the more negatively charged perlite surface can more easily take place:

$$-\mathrm{SiOH} + \mathrm{Cu}^{2+} \rightleftharpoons \mathrm{SiO}{-}\mathrm{Cu}^+ + \mathrm{H}^+. \qquad [1]$$

Ionic strength affects the activity coefficients for OH^-, H_3O^+, and specifically adsorbable ions. As seen in Fig. 5, increasing the ionic strength of solution causes a decrease in adsorption of Cu^{2+} ions onto perlite surfaces. This indicates that the negative charge of the surface of perlite, which has no pH_{pzc} in the range of pH 3–11 (42–44), decreases with increasing ionic strength, resulting in reducing the adsorption capacity.

A study of the temperature dependence of adsorption reactions gives valuable information about the enthalpy change during adsorption. Greater adsorption is often found at lower temperatures, but the differences are usually small. The effect of temperature on the adsorption isotherm was studied by carrying out a series of isotherms at 30, 40, 50, and 60°C for both of the perlite samples (unexpanded perlite and expanded perlite), as shown in Fig. 6. Results indicate that the adsorption capacity of unexpanded and expanded perlite for Cu^{2+} decreases with increase in temperature. The effect of temperature is fairly common and increasing temperature results in an increase in the rate of approach to equilibrium. In addition, the temperature coefficient for the reverse reaction is greater than for the forward reaction and consequently the equilibrium capacity decreases with increased temperature (55).

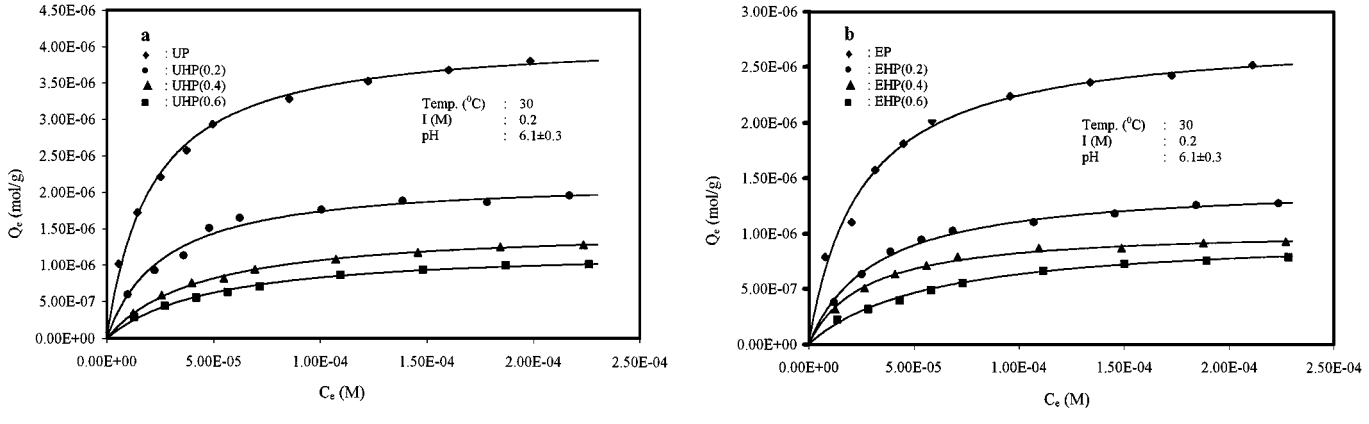

FIG. 3. The effect of acid activation on the adsorption of Cu^{2+} ions on perlite: (a) UP and (b) EP.

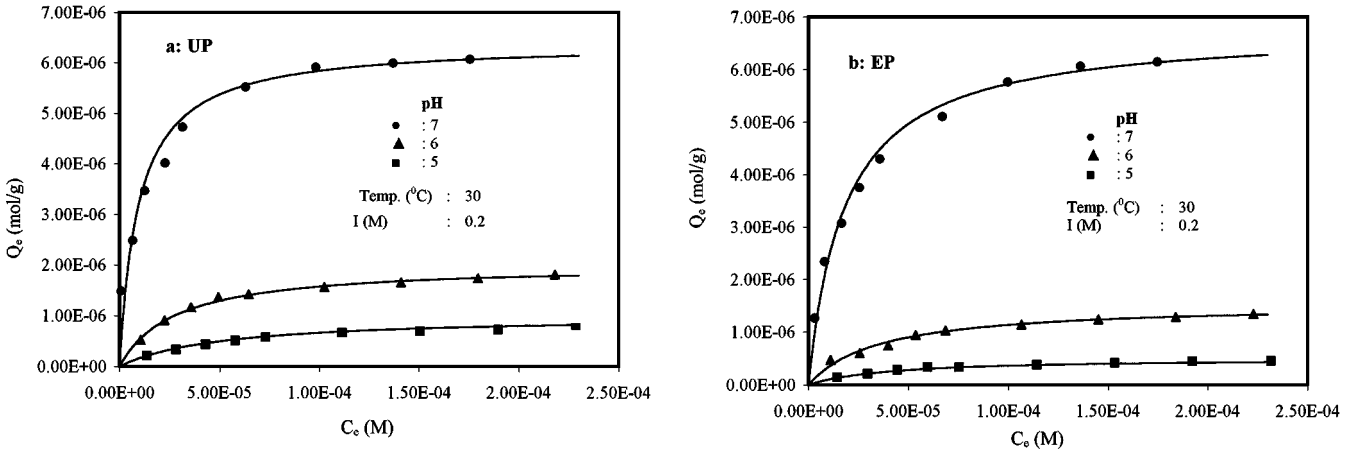

FIG. 4. The effect of solution pH on the adsorption of Cu^{2+} ions on perlite: (a) UP and (b) EP.

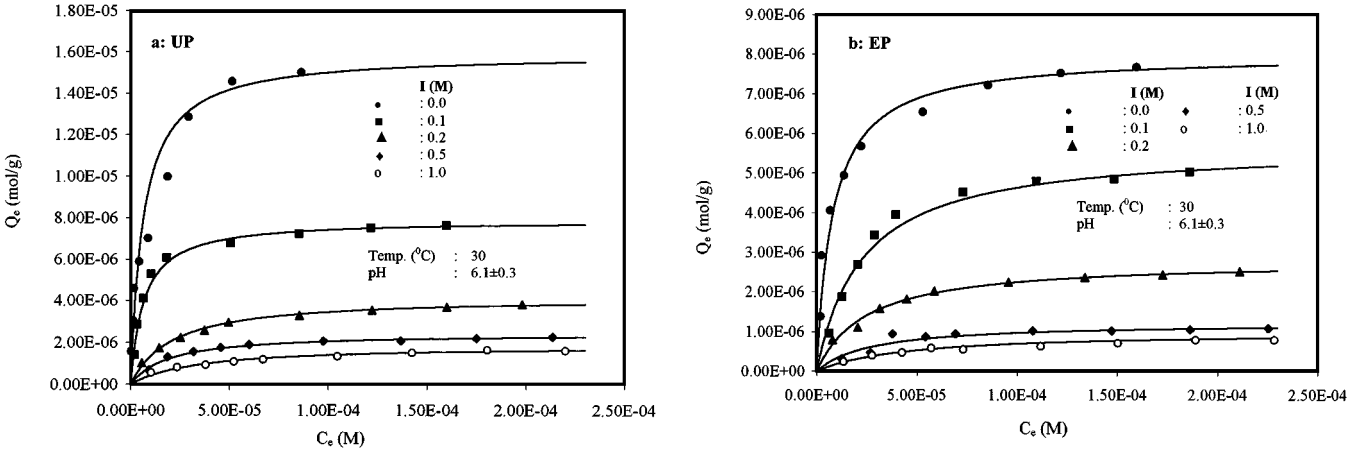

FIG. 5. The effect of ionic strength on the adsorption of Cu^{2+} ions on perlite: (a) UP and (b) EP.

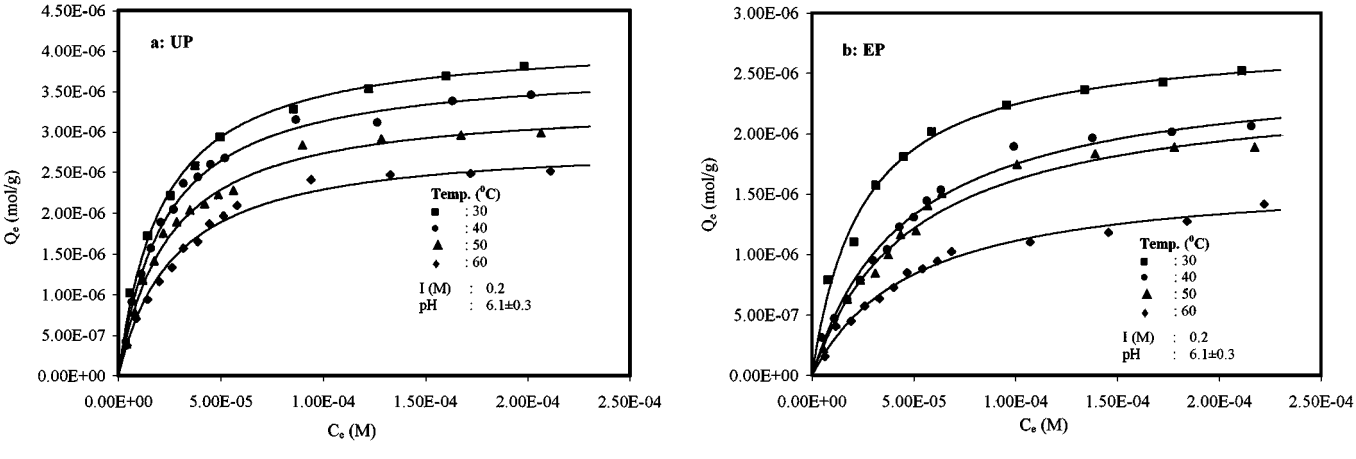

FIG. 6. The effect of temperature on the adsorption of Cu^{2+} ions on perlite: (a) UP and (b) EP.

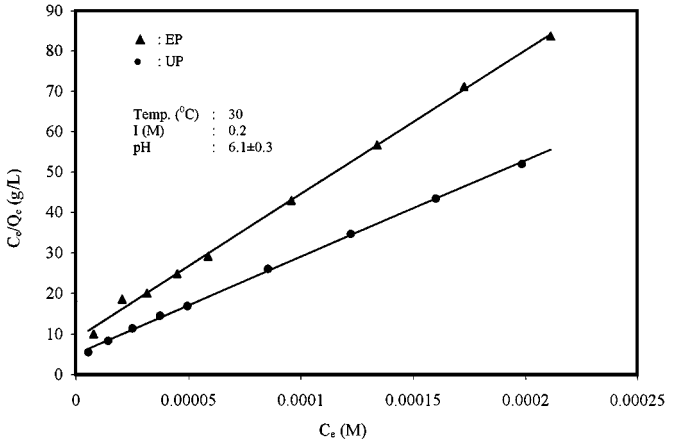

FIG. 7. Langmuir adsorption isotherm for data of Fig. 2.

3.3. Isotherm Analysis

The equilibrium adsorption isotherm is of fundamental importance in the design of adsorption systems. The Langmuir equation, which is valid for monolayer adsorption onto a surface containing a finite number of identical sites, is the equation most frequently used to represent data on adsorption from solution. The exact shape of the adsorption isotherm for a heterogeneous adsorbent will depend on the distribution of the K values or, more specifically, on the frequency distribution of the adsorption energy sites on the adsorbent (44, 45).

The Langmuir equation can be expressed as

$$Q_e = \frac{Q_m K C_e}{1 + K C_e}$$

or

$$\frac{C_e}{Q_e} = \frac{1}{Q_m K} + \frac{C_e}{Q_m}, \qquad [11]$$

where Q_m = the maximum surface coverage representing the formation of a monomolecular layer on the surface of the adsorbent (mol g^{-1}), Q_e = equilibrium Cu(II) concentration on adsorbent (mol g^{-1}), C_e = the equilibrium Cu(II) concentration in solution (mol L^{-1}), and K = adsorption constant (L mol^{-1}).

According to the Freundlich equation, the amount of substance adsorbed per gram of adsorbent (Q_e) is related to the equilibrium concentration (C_e) by the equation

$$Q_e = K_F C_e^{1/n}$$

or

$$\ln Q_e = \ln K_F + \frac{1}{n} \ln C_e, \qquad [12]$$

where K_F and n are empirical constants. The values of n is usually between 2 to 10 (56).

According to Eq. [11], a plot of C_e/Q_e versus C_e should be a straight line with a slope $1/Q_m$ and intercept $1/Q_m K$ when adsorption follows the Langmuir equation. If it follows the Freundlich equation, a plot of log Q_e against log C_e should give a straight line, of slope $1/n$ and of intercept log K_F. The straight lines shown in Figs. 7–11 show that Eq. [11] can adequately represent the adsorption process. Adsorption isotherms were obtained in terms of Eqs. [11] and [12] by using experimental adsorption results in these equations. Values for Q_m, K, n, and K_F are summarized in Table 4. The isotherm data were calculated from the least-squares method and the related correlation coefficients (r values) are given in the same table. As seen from the Table 4, the Langmuir equation represents the adsorption process very well; the r values were almost all higher than 0.99, indicating a very good mathematical fit. The fact that the Langmuir isotherm fits the experimental data very well may be due to homogenous distribution of active sites on the perlite surface, since the Langmuir equation assumes that the surface is homogenous (44, 45).

The shape of the isotherm may also be considered with a view to predicting if an adsorption system is "favorable"

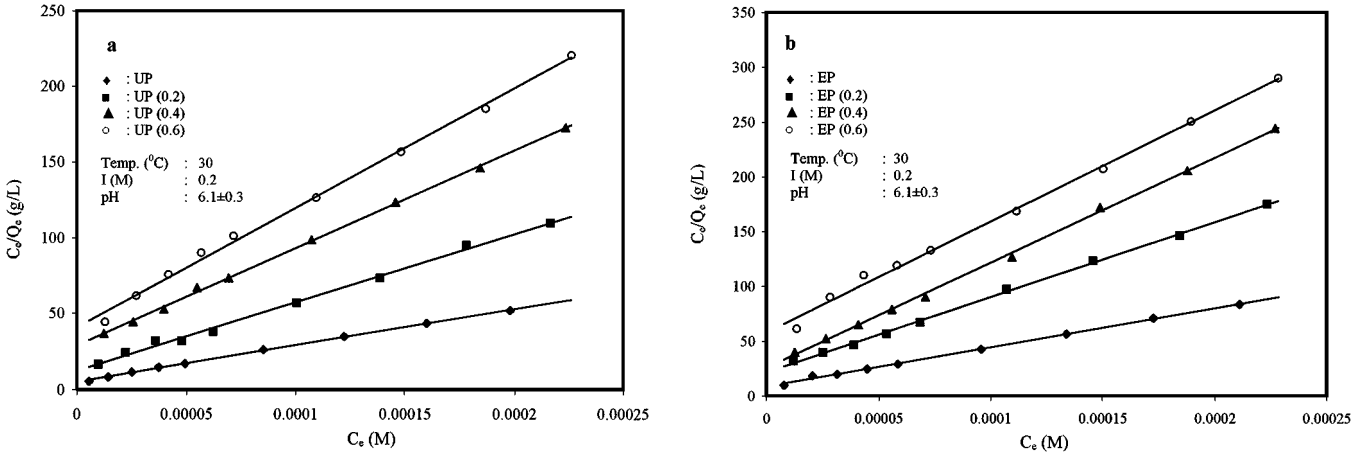

FIG. 8. Langmuir adsorption isotherm for data of Fig. 3: (a) UP and (b) EP.

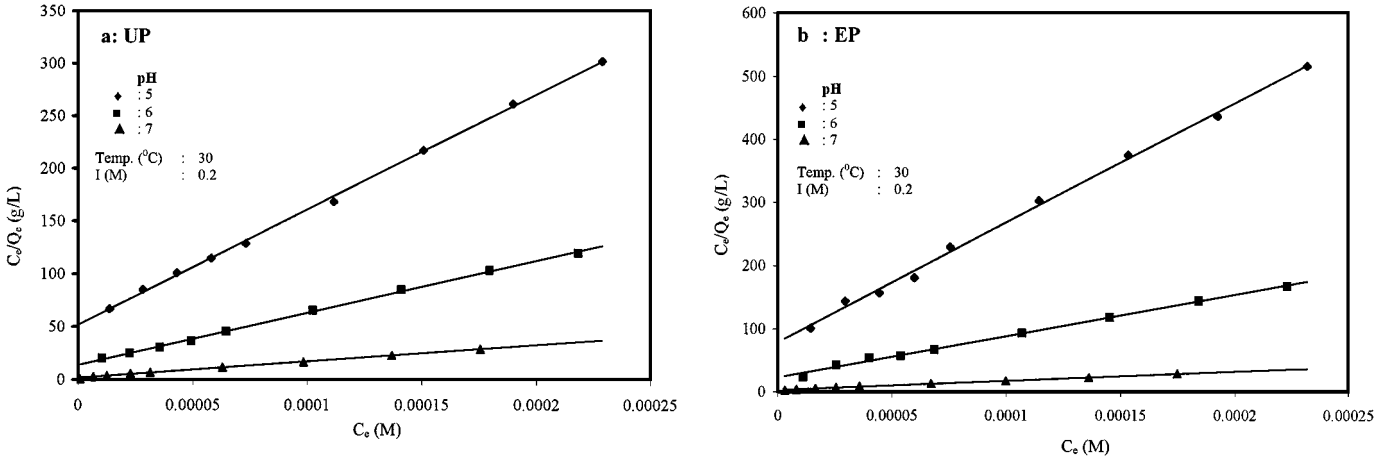

FIG. 9. Langmuir adsorption isotherm for data of Fig. 4: (a) UP and (b) EP.

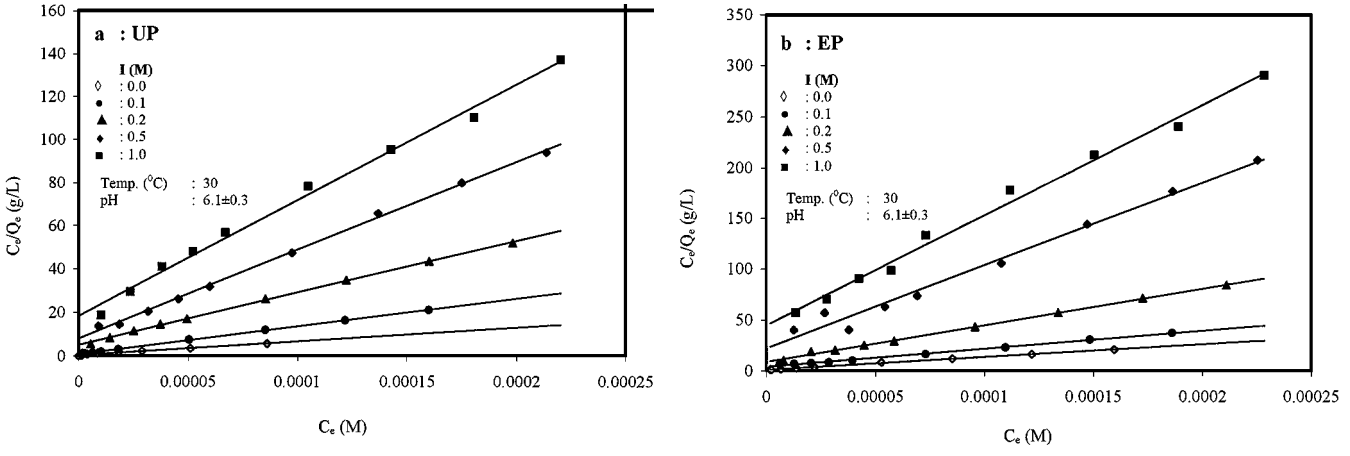

FIG. 10. Langmuir adsorption isotherm for data of Fig. 5: (a) UP and (b) EP.

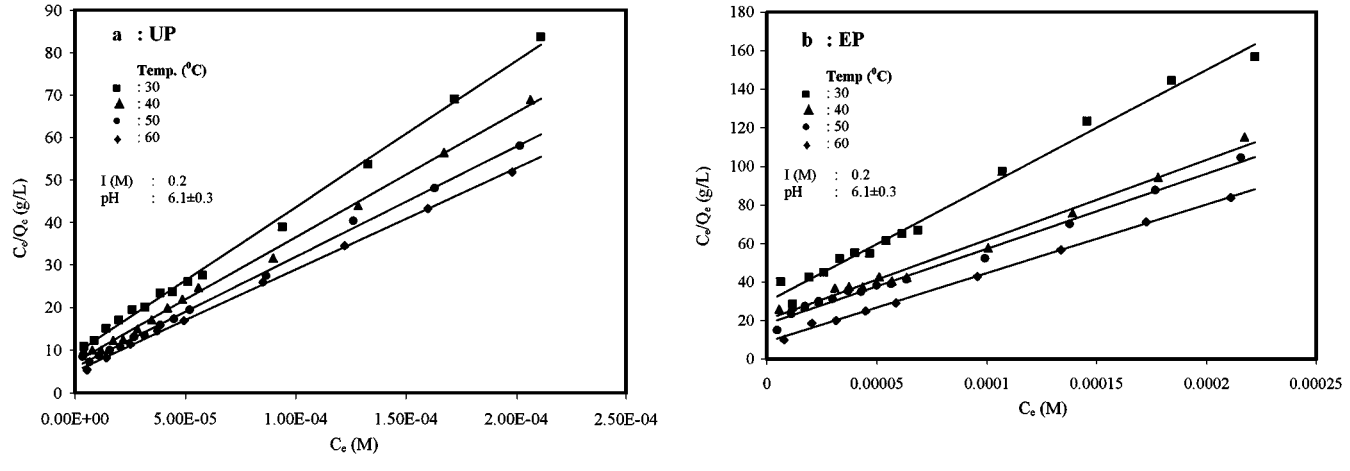

FIG. 11. Langmuir adsorption isotherm for data of Fig. 6: (a) UP and (b) EP.

TABLE 4
Langmuir Isotherm Constants for Perlite Samples

Sample	Temperature (°C)	I (M)	pH	Langmuir isotherm $Q_m \times 10^6$ (mol/g)	Langmuir isotherm $K \times 10^{-4}$ (L/mol)	Langmuir isotherm r	Freundlich isotherm n	Freundlich isotherm $K_F \times 10^5$	Freundlich isotherm r	R
UP	30	0.2	6.1 ± 0.3	4.17	4.75	0.9996	2.81	8.87	0.9749	0.791–0.096
UHP(0.2)	30	0.2	6.1 ± 0.3	2.21	3.73	0.9981	2.64	5.44	0.9562	0.733–0.110
UHP(0.4)	30	0.2	6.1 ± 0.3	1.55	2.26	0.9995	2.26	5.91	0.9754	0.782–0.165
UHP(0.6)	30	0.2	6.1 ± 0.3	1.26	1.96	0.9982	2.25	4.70	0.9916	0.822–0.207
EP	30	0.2	6.1 ± 0.3	2.80	4.04	0.9990	2.79	5.82	0.9683	0.759–0.105
EHP(0.2)	30	0.2	6.1 ± 0.3	1.46	3.16	0.9995	2.57	3.79	0.9552	0.726–0.124
EHP(0.4)	30	0.2	6.1 ± 0.3	1.04	3.76	0.9994	2.83	2.03	0.9519	0.679–0.105
EHP(0.6)	30	0.2	6.1 ± 0.3	1.00	1.73	0.9978	2.15	4.30	0.9901	0.810–0.202
UP	30	0.2	5	1.00	1.93	0.9995	2.21	3.80	0.9752	0.791–0.185
UP	30	0.2	6	2.02	3.59	0.9994	2.66	4.79	0.9527	0.725–0.113
UP	30	0.2	7	6.39	10.52	0.9989	3.55	7.83	0.9853	0.912–0.051
EP	30	0.2	5	0.50	2.54	0.9986	2.47	1.47	0.9718	0.733–0.145
EP	30	0.2	6	1.52	2.88	0.9978	2.76	3.02	0.9832	0.759–0.135
EP	30	0.2	7	6.78	5.48	0.9989	2.61	19.52	0.9791	0.853–0.095
UP	30	0.0	6.1 ± 0.3	15.94	16.13	0.9936	2.97	38.13	0.9021	0.990–0.067
UP	30	0.1	6.1 ± 0.3	7.91	15.39	0.9998	3.20	14.15	0.9878	0.786–0.039
UP	30	0.2	6.1 ± 0.3	4.17	4.75	0.9996	2.81	8.87	0.9749	0.791–0.096
UP	30	0.5	6.1 ± 0.3	2.45	5.15	0.9991	3.00	4.28	0.9197	0.681–0.083
UP	30	1.0	6.1 ± 0.3	1.86	2.95	0.9967	2.82	3.44	0.9935	0.768–0.133
EP	30	0.0	6.1 ± 0.3	7.98	12.44	0.9993	3.21	13.66	0.9148	0.803–0.048
EP	30	0.1	6.1 ± 0.3	5.69	4.38	0.9979	2.25	28.19	0.9305	0.788–0.109
EP	30	0.2	6.1 ± 0.3	2.80	4.04	0.9990	2.79	5.82	0.9683	0.759–0.105
EP	30	0.5	6.1 ± 0.3	1.22	3.69	0.9924	2.54	3.50	0.8723	0.683–0.107
EP	30	1.0	6.1 ± 0.3	1.00	2.25	0.9960	2.52	2.40	0.9698	0.769–0.163
UP	30	0.2	6.1 ± 0.3	4.17	4.75	0.9996	2.81	8.87	0.9749	0.791–0.096
UP	40	0.2	6.1 ± 0.3	3.84	4.41	0.9988	2.16	23.17	0.9357	0.774–0.101
UP	50	0.2	6.1 ± 0.3	3.39	4.15	0.9986	2.15	20.63	0.9372	0.754–0.105
UP	60	0.2	6.1 ± 0.3	2.89	3.78	0.9984	2.13	17.65	0.9568	0.753–0.111
EP	30	0.2	6.1 ± 0.3	2.80	4.04	0.9990	2.79	5.82	0.9683	0.759–0.105
EP	40	0.2	6.1 ± 0.3	2.56	2.15	0.9951	1.89	22.23	0.9805	0.808–0.177
EP	50	0.2	6.1 ± 0.3	2.41	2.03	0.9944	1.72	34.12	0.9630	0.811–0.185
EP	60	0.2	6.1 ± 0.3	1.66	2.02	0.9941	1.86	15.58	0.9537	0.809–0.182

or "unfavorable." The essential characteristic of a Langmuir isotherm can be expressed in terms of a dimensionless separation factor or equilibrium parameter R (57), which is defined by relationship

$$R = \frac{1}{1 + KC_e}. \qquad [13]$$

According to the value of R the isotherm shape may be interpreted as follows:

Value of R	Type of adsorption
$R > 1.0$	Unfavorable
$R = 1.0$	Linear
$0 < R < 1.0$	Favorable
$R = 0$	Irreversible

The results given in Table 4 show that the adsorption of Cu^{2+} ion on the perlite is favorable.

From the adsorption data at various temperatures, the enthalpy change for Cu^{2+} adsorption can be estimated from the van't Hoff isochore (58, 59):

$$\left[\frac{\partial \ln K}{\partial T}\right]_\theta = \frac{\Delta H_{ads}}{R_g T^2}. \qquad [14]$$

The subscript θ means that the equilibrium constant at each temperature is measured at constant coverage. Under these conditions, from the Langmuir equation at $\theta = 0.5$, $K = 1/C_e$ and so

$$\left[\frac{\ln C_e}{(1/T)}\right]_{\theta=0.5} = \frac{\Delta H_{ads}}{R_g}, \qquad [15]$$

where R_g is the gas constant.

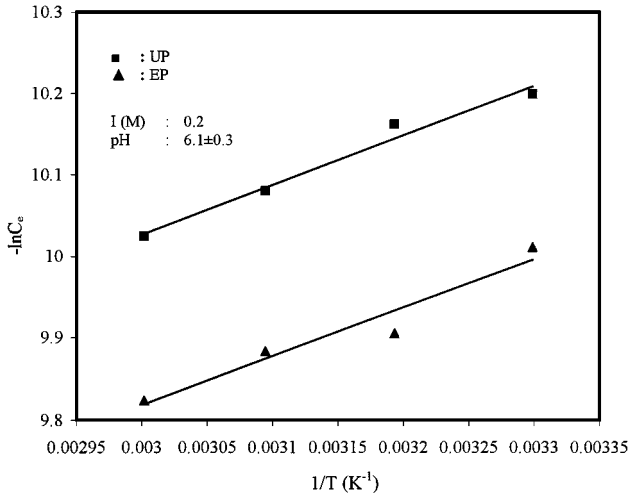

FIG. 12. Plot of $-\ln C_e$ versus $1/T$ for Cu^{2+} ion adsorption on perlite.

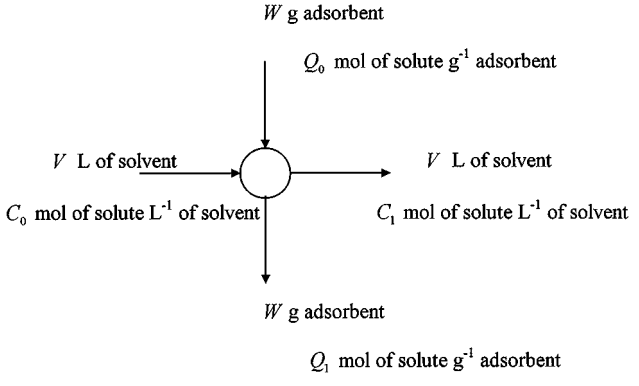

FIG. 13. Single stage batch adsorber.

This value of ΔH_{ads} is called the isosteric heat of adsorption referring to the fact that it applies to a certain value of the coverage. The Langmuir model implies that ΔH_{ads} should be constant, but it is more likely to be a function of coverage ($\theta = Q_e/Q_m$).

The values of ΔH_{ads} were calculated as -4.38 ± 1 kJ/mol for expanded perlite and -5.14 ± 1 kJ/mol for unexpanded perlite from the data given in Fig. 12 according to Eq. [15]. The results show that the interactions between surface and adsorbate molecules are weak enough to be considered as van der Waals forces.

3.4. Designing Batch Adsorption from Isotherm Data

Adsorption isotherms can be used to predict the design of single stage batch adsorption systems (60). A schematic diagram is shown in Fig. 13, where the effluent contains V liters of water and an initial metal ion concentration C_0, which is to be reduced to C_1 in the adsorption process. In the treatment stage Wg perlite (Cu^{2+}-free) is added and the Cu^{2+} concentration on the solid changes from $Q_0 = 0$ (initially) to Q_1. The mass balance that equates the Cu^{2+} removed from the liquid effluent to that accumulated by the solid is

$$V(C_0 - C_1) = W(Q_1 - Q_0) = WQ_1. \qquad [16]$$

In the case of the adsorption of Cu^{2+} on unexpanded and expanded perlite samples the Langmuir isotherm gives the best fit to experimental data. Consequently Q_e from Eq. [11] can be best substituted for Q_1 in the rearranged form of Eq. [16], giving adsorbent/solution ratios for this particular system:

$$\frac{W}{V} = \frac{C_0 - C_1}{Q_e} \equiv \frac{C_0 - C_e}{\left(\frac{Q_m K C_e}{1 + K C_e}\right)}. \qquad [17]$$

Figures 14a and b show a series of plots derived from Eq. [17] for the adsorption of Cu^{2+} on unexpanded and expanded perlite.

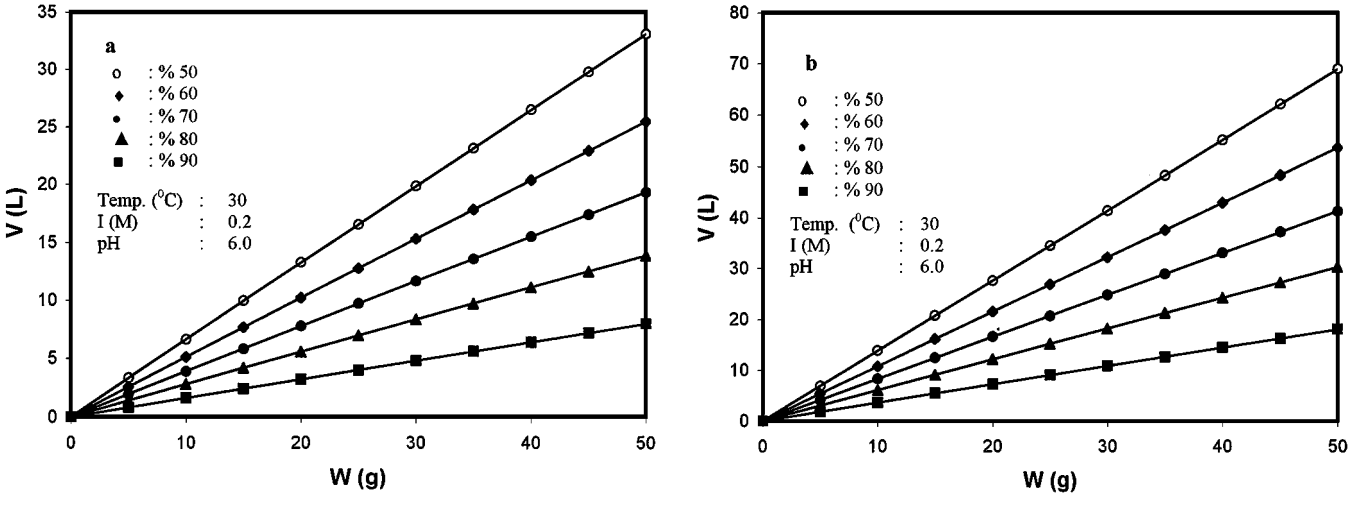

FIG. 14. Volume of effluent (V) treated against adsorbent mass (W) for different percentages of Cu^{2+} removal: (a) UP and (b) EP.

An initial Cu^{2+} concentration of 1.6×10^{-5} mol/L is assumed, and the figures show the amount of effluent which can be treated to reduce the Cu^{2+} content by 50, 60, 70, 80, and 90% using various masses of adsorbent.

4. CONCLUSIONS

The following points may be mentioned as the results of this study:

1. It has been found that the number of protons released per Cu^{2+} ion adsorbed onto perlite samples was about 1 for both the unexpanded and expanded perlites.
2. The experimental data were correlated reasonably well by the Langmuir adsorption isotherm and the isotherm parameters (Q_m and K) have been calculated.
3. The adsorbed amount of Cu^{2+} ions slightly decreased with increasing concentration of H_2SO_4 used for the acid activation for both perlite samples.
4. The adsorbed amounts of Cu^{2+} ions increased with increasing pH for both perlite samples.
5. The adsorbed amount of Cu^{2+} ions slightly decreased with increase in ionic strength for both perlite samples.
6. The adsorbed amount of Cu^{2+} ions decreased with increase in temperature for both perlite samples.
7. The dimensionless separation factor (R) showed that perlite can be used for removal of Cu^{2+} ions from aqueous solutions, but unexpanded perlite is more effective. Its adsorption capacity is greater than that of expanded perlite.
8. The values of ΔH_{ads} for unexpanded and expanded perlite samples were calculated as -5.14 ± 1 and -4.38 ± 1 kJ/mol, respectively.
9. Perlite has considerable potential as an adsorbent of metal ions in a commercial system because of being cheap.

APPENDIX: NOMENCLATURE

Q_m	Monolayer capacity of the adsorbent, mol g^{-1}
K	Adsorption constant, g mol^{-1}
C_e	Equilibrium metal ion concentration in solution, mol L^{-1}
Q_e	Equilibrium metal ion concentration on adsorbent, mol g^{-1}
K_F	Freundlich isotherm constant
n	Freundlich isotherm constant
R	Dimensionless separation factor
ΔH_{ads}	Heat of adsorption, kJ mol^{-1}
T	Temperature, K
W	Mass of adsorbent, g
V	Volume of aqueous solution to be treated, L
C_0	Initial metal ion concentration in aqueous solution, mol L^{-1}
x	Proton stoichiometry

ACKNOWLEDGMENT

The work was financially supported by Balıkesir University Research Fund (Project 2000/1).

REFERENCES

1. Bereket, G., Aroğuz, A. Z., and Özel, M. Z., *J. Colloid Interface Sci.* **187,** 338 (1997).
2. Irwing Sax, N., "Handbook of Dangerous Materials," pp. 218–222, 236. Reinhold, New York, 1951.
3. Gonzales-Davila, M., Santana-Casino, J. M., and Millero, F. J., *J. Colloid Sci.* **137** (1990).
4. Huang, C. D., and Blankenship, D. W., *Water Res.* **18,** 37 (1984).
5. Naylor, L. M., and Daugue, R. R., *J. Am. Water Works Assoc.* **67,** 560 (1975).
6. Kahashi, Y. Y., and Imai, H., *Soil Sci. Plant Nutr.* **29,** 111 (1983).
7. Battacharya, A. K., and Venkobachor, *J. Environ. Eng.* **110,** 110 (1984).
8. Tewari, P. H., Campbell, A. B., and Lee, W., *Can. J. Chem.* **50,** 1642 (1972).
9. Tewari, P. H., and Lee, W., *J. Colloid Interface Sci.* **52,** 77 (1975).
10. Baumgarten, E., and Kirchhausen-Düsing, U., *J. Colloid Interface Sci.* **194,** 1 (1997).
11. Tamura, H., Matijevic, E., and Meites, L., *J. Colloid Interface Sci.* **92,** 303 (1983).
12. Fokkink, L. G. J., De Keizer, A., and Lyklema, J., *J. Colloid Interface Sci.* **135,** 118 (1990).
13. Gray, M. J., and Malati, M. A., *J. Chem. Technol. Biotechnol.* **29,** 135 (1979).
14. Malati, M. A., McEvoy, M., and Harvey, C. R., *Surf. Technol.* **17,** 165 (1982).
15. Bye, G. C., McEvoy, M., and Malati, M. A., *J. Chem. Technol. Biotechnol.* **32,** 781 (1982).
16. Bye, G. C., McEvoy, M., and Malati, M. A., *J. Chem. Soc. Faraday Trans. 1* **79,** 2311 (1983).
17. Kosmulski, M., *J. Colloid Interface Sci.* **195,** 395 (1997).
18. Kosmulski, M., *J. Colloid Interface Sci.* **211,** 410 (1999).
19. Bruemmer, G. W., Gerth, J., and Tiller, K. G., *J. Soil. Sci.* **39,** 37 (1988).
20. Johnson, B. B., *Environ. Sci. Technol.* **24,** 112 (1990).
21. Rodda, D. P., Johnson, B. B., and Wells, J. D., *J. Colloid Interface Sci.* **161,** 57 (1993).
22. Angove, M. J., Wells, J. D., and Johnson, B. B., *J. Colloid Interface Sci.* **211,** 281 (1999).
23. Rodda, D. P., Wells, J. D., and Johnson, B. B., *J. Colloid Interface Sci.* **184,** 564 (1996).
24. Kobal, I., Hesleitner, P., and Matijevic, E., *Colloids Surf.* **33,** 167 (1988).
25. Srivastava, A., and Srivastava, P. C., *Environ. Pollut.* **68,** 171 (1990).
26. İnel, O., and Kayıkçı, N., *Doğa-TR.T. of Engineering and Environmental Sciences*, 332 (1990).
27. Onganer, Y., and Temur, Ç., *J. Colloid Interface Sci.* **205,** 241 (1998).
28. Zhang, Q., Xu, Z., and Finch, *J. A., J. Colloid Interface Sci.* **175,** 61 (1995).
29. Zhang, Q., Xu, Z., and Finch, J. A., *J. Colloid Interface Sci.* **169,** 414 (1995).
30. Ludwing, C., and Schindler, P. W., *J. Colloid Interface Sci.* **169,** 284 (1995).
31. Yang, J.-K., and Davis, A. P., *J. Colloid Interface Sci.* **216,** 77 (1999).
32. Apak, R., Güçlü, K., and Turgut, M. H., *J. Colloid Interface Sci.* **203,** 122 (1998).
33. Güçlü, K., and Apak, R., *J. Colloid Interface Sci.* **228,** 238 (2000).
34. Farquhar, M. L., Charnock, J. M., England, K. E. R., and Vaughan, D. J., *J. Colloid Interface Sci.* **177,** 561 (1996).
35. Du, Q., Sun, Z., Forsling, W., and Tang, H., *J. Colloid Interface Sci.* **187,** 232 (1997).
36. Angove, M. J., Johnson, B. B., and Wells, J. D., *J. Colloid Interface Sci.* **204,** 93 (1998).
37. Schlegel, M. L., Manceau, A., Chateigner, D., and Charlet, L., *J. Colloid Interface Sci.* **215,** 140 (1999).

38. Harben, P. W., and Bates, R. L., “Industrial Minerals Geology and World Deposits,” p. 184. Metal Bulletin Inc., London, 1990.
39. Anonymous, *Market Anal.* **11** (May 1969).
40. Uluatam, S. S., *J. Am. Water Works Assoc.* **70** (June 1991).
41. Chesterman, C. W., “Industrial Minerals and Rocks,” 4th Ed., p. 927. AIME, New York, 1975.
42. Doğan, M., Alkan, M., and Çakir, Ü., *J. Colloid Interface Sci.* **192,** 114 (1997).
43. Alkan, M., and Doğan, M., *J. Colloid Interface Sci.* **207,** 90 (1998).
44. Doğan, M., Alkan, M., and Onganer, Y., *Water, Air, Soil Pollut.* **120,** 229 (2000).
45. Kinniburgh, D. G., *in* “Adsorption of Inorganic Solid–Liquid Interfaces” (M. A. Anderson and A. J. Rubin, Eds.), pp. 91–160. Ann Arbor Science Publisher, Ann Arbor, MI, 1981.
46. Kanungo, S. B., *J. Colloid Interface Sci.* **162,** 93 (1994).
47. Müller, B., and Sigg, L., *J. Colloid Interface Sci.* **148,** 517 (1991).
48. Fokkink, L. G. J., DeKeizer, A., and Lyklema, L., *J. Colloid Interface Sci.* **118,** 454 (1987).
49. Park, Y. J., Junk, K.-H., and Park, K. K., *J. Colloid Interface Sci.* **172,** 447 (1995).
50. Bourg, A. C. M., and Schindler, P. W., *Chimia* **32,** 166 (1978).
51. Balistrieri, L. S., and Murray, J. W., *Geochim. Cosmochim. Acta* **47,** 1091 (1983).
52. Gonzàlez-Pradas, E., Villafranca-Sànchez, M., Valverde-Garcìa, A., and Socias-Viciana, M., *J. Chem. Tech. Biotechnol.* **42,** 105 (1988).
53. López-Gonzàlez, J. D., and Gonzàlez-Garcìa, S., *An. Fis. Quim. Ser. B* **50,** 465 (1954).
54. Doğan, M., M. Sc. Thesis, University of Balıkesir Faculty of Science and Literature, Balıkesir, Turkey, 1997 [in Turkish].
55. Mac Kay, G., and McConvey, I. F., *Chem. Eng. Process,* **19,** 287 (1985).
56. Laidler, K. J., and Meiser, J. H., “Physical Chemistry,” p. 852. Houghton Mifflin, New York, 1999.
57. Gonzàlez-Pradas, E., Villafranca-Sànchez, M., Socias-Viciana, M., del-Rey-Bueno, F., and Garcìa-Rodriguez, A., *J. Chem. Tech. Biotechnol,* **39,** 19 (1987).
58. McKay, G., Otterburn, M. S., and Aga, A. J., *Water, Air, Soil Pollut.* **24,** 307 (1985).
59. Hunter, R. J., “Introduction to Modern Colloid Science,” p. 168. Oxford, Sci. Pub, Oxford, England (1999).
60. McKay, G., and Poots, V. J. P., *J. Chem. Tech. Biotechnol.* **30,** 279 (1980).